

Practical method for treating the Coulomb force in momentum space

Kazumi Kume and Kenji Kume

Department of Physics, Nara Women's University, Nara 630-8506, Japan

(Received 17 September 1998)

We propose a practical numerical method for treating the Coulomb interaction in momentum space. The Coulomb potential is regularized by expanding its inner part $r \leq R$ as the superposition of the Gaussian functions. This smooth-cutoff Coulomb potential decreases rapidly in momentum space without oscillation. In addition, the partial-wave decomposition can be done analytically without numerical integration. First, the phase shifts are calculated with the regularized Coulomb plus short-range strong potentials. Then, the correct phase shifts or the wave functions can be reconstructed with the aid of coordinate-space calculation from the asymptotic region inward to R . Another possibility is to calculate the logarithmic derivative at R directly by the Fourier transform, which is matched to the point-Coulomb wave functions F_L and G_L . This method is examined for calculating the phase shifts of proton-nucleus elastic scattering and found to be accurate over wide energy regions. [S0556-2813(99)01904-4]

PACS number(s): 24.10.-i, 02.60.Nm, 25.40.-h, 25.70.-z

I. INTRODUCTION

A momentum-space method for solving wave equations such as Schrödinger, Dirac or Klein-Gordon equations has been extensively used for scattering or bound-state problems. When the scattering phenomena are precisely described, a nonlocal interaction often appears, for example, in pion-nucleus and proton-nucleus elastic scatterings, or heavy-ion collisions. In such cases, it is natural and advantageous to solve the wave equation in momentum space. In the momentum-space calculation, however, the singularity associated with the long-range Coulomb force causes numerical difficulty. There have been various attempts to avoid this [1]. Approximately 25 years ago, Vincent and Phatak (VP) proposed a procedure to treat the Coulomb interaction in momentum space [1] whereby the long-range Coulomb potential is regularized by cutting it off at radius R , where short-range interaction is negligible and the Coulomb potential takes its point value $Z_1 Z_2 e^2 / r$. From the phase shifts $\delta_L^{(0)}$, the coordinate-space wave function can be calculated at radius R , which is smoothly matched to the Coulomb wave function reproducing the correct phase shifts δ_L . This procedure has been extensively applied to the calculation of scattering-state [2,3] and to solving bound-state problems [4] in momentum space. The VP procedure was originally developed to treat the Coulomb interaction in the pion-nucleus scattering at intermediate energy. To be used on proton-nucleus elastic scattering, where large momentum transfer is involved, the VP procedure needs to be improved to achieve better accuracy. Recently, several modifications and/or approximations of the VP procedure have been examined concerning the study of proton-nucleus elastic scattering. Crespo and Tostevin [5] and Picklesimer *et al.* [6] suggested the approximate algorithms to reduce the numerical errors. Arellano *et al.* [7] used a somewhat simplified nuclear charge distribution [8] to obtain the accurate Coulomb matrix elements. In addition, the Coulomb force in the multiple scattering [9] or angular-momentum states coupled by an optical potential [10] have been studied.

Even though the original VP prescription is correct, in

principle, it is difficult to obtain satisfactory accuracy with this method, especially for the proton-nucleus scattering, in which the high- q Coulomb matrix element plays an important role. There are mainly two reasons for this. First, the sharp-cutoff Coulomb potential, which rapidly oscillates in momentum space, involves a large high- q component which brings numerical errors when solving the integral equation. Second, the partial wave decomposition of the momentum-space Coulomb potential is numerically difficult due to rapid oscillation as a function of momentum transfer q . To avoid these difficulties, Ottenstein *et al.* [11,12] proposed an improved method in which the Coulomb potential is shielded by introducing the Gaussian-type charged shell outside the range of the strong potential. Though their regularized Coulomb potential decreases rapidly in momentum space, there still remains a small but non-negligible rapidly oscillating component. In addition, the partial-wave decomposition has to be carried out numerically, possibly causing numerical errors.

An alternative method using the point Coulomb function as the basis set has also been considered [13,14]. In that method, however, the matrix elements of the short-range force has to be calculated with respect to the Coulomb wave function. These matrix elements are not easy to calculate because the short-range force is often given in the momentum representation. Another method using screened Coulomb interaction is proposed and used in the context of few-body physics [15,16].

In the present paper, we propose a simple and accurate method to treat the Coulomb interaction in momentum space which is free from the above difficulties in the VP method. Our method is basically a modification of the VP procedure. By expanding the inner region of the Coulomb potential ($r \leq R$) as a superposition of the Gaussian functions with various ranges, we can smoothly regularize the Coulomb potential. Being represented as the sum of Gaussian functions, the partial-wave decomposition can be done analytically. In addition, the oscillatory high- q component is eliminated. The correct phase shifts or wave function can be reconstructed with the aid of coordinate-space calculation from the

asymptotic region inward to R , as in the method of Ottenstein *et al.* [11,12], or by directly calculating the logarithmic derivative at R by the Fourier transform, which is matched to the Coulomb wave function. Our method overcomes the above mentioned difficulties inherent in the original VP procedure and yields accurate numerical results. When tested for proton-nucleus elastic scattering, the algorithm proves to be accurate over the wide energy region.

II. ALGORITHM AND RESULTS

To explain our method, we restricted ourselves to the case of the nonrelativistic Schrödinger equation for proton-nucleus elastic scattering

$$(k_0^2 - k^2)\psi(\mathbf{k}) = 2M \int [U(\mathbf{k}, \mathbf{k}') + V(\mathbf{k}, \mathbf{k}')] \psi(\mathbf{k}') d\mathbf{k}', \quad (1)$$

where $U(\mathbf{k}, \mathbf{k}')$ is the short-range strong potential and $V(\mathbf{k}, \mathbf{k}')$ is the proton-nucleus Coulomb potential in momentum representation. This equation should be solved with an appropriate scattering boundary condition. The Coulomb potential is given as

$$V(\mathbf{k}, \mathbf{k}') = \frac{Ze^2}{2\pi^2} \frac{\rho(q)}{q^2} \quad (2)$$

with

$$\mathbf{q} = \mathbf{k} - \mathbf{k}', \quad (3)$$

where Ze is the nuclear charge. The nuclear charge form factor $\rho(q)$ is normalized to $\rho(0) = 1$. The original VP procedure is to regularize the Coulomb potential by cutting it off sharply at radius R . Then it becomes

$$\frac{Ze^2}{2\pi^2} \frac{\rho(q) - \cos qR}{q^2}. \quad (4)$$

Because of the factor $\cos qR$ in above equation, this potential rapidly oscillates and slowly decreases at the high- q region. To avoid this, Ottenstein *et al.* [11,12] introduced the negatively charged shell outside the nucleus, which smoothly shields the long-range Coulomb potential. They used the Gaussian-type charged shell located around R_{sh}

$$\rho(r) = \rho_0 \exp\left[-\left(\frac{r - R_{\text{sh}}}{a_{\text{sh}}}\right)^2\right] \quad (5)$$

with $\rho_0 = -Ze/[4\pi^{3/2}a_{\text{sh}}(a_{\text{sh}}^2/2 + R_{\text{sh}}^2)]$. Then the shielded Coulomb potential becomes

$$\frac{1}{2\pi^2} \frac{Ze^2}{q^2} \left\{ \rho(q) - \frac{1}{1+\beta} \left(\cos qR_{\text{sh}} + \beta \frac{\sin qR_{\text{sh}}}{qR_{\text{sh}}} \right) \times \exp\left[-\frac{a_{\text{sh}}^2 q^2}{4}\right] \right\} \quad (6)$$

with $\beta = 2(R_{\text{sh}}/a_{\text{sh}})^2$. In this potential, the second term still oscillates very rapidly because of factors $\cos qR_{\text{sh}}$ or $\sin qR_{\text{sh}}$. Due to the exponential factor $\exp[-a_{\text{sh}}^2 q^2/4]$, the

second term itself decreases rapidly. We should take the parameters R_{sh} and a_{sh} such that the negatively charged shell does not overlap with the short-range potential. This requires that the strong potential be negligible at $r \geq R_{\text{sh}} - 4a_{\text{sh}}$. We should also take a sufficiently large a_{sh} value. Otherwise, the oscillating second term in Eq. (6) dominates, and the regularized Coulomb potential exhibits highly oscillatory behavior. In the practical calculation, the second term is non-negligible. Moreover, the partial-wave decomposition of this shielded potential has to be carried out with care.

To overcome these difficulties, we propose to expand the Coulomb potential approximately with the Gaussian functions within radius R

$$V(r) \approx \sum_{i=1}^N c_i \exp[-\lambda_i r^2] \quad (0 \leq r \leq R), \quad (7)$$

where the radius R is chosen such that the short-range potential is negligible and the Coulomb potential takes its point value at $r \geq R$. Then, the resulting regularized potential

$$\bar{V}(r) = \sum_{i=1}^N c_i \exp[-\lambda_i r^2] \quad (0 \leq r < \infty), \quad (8)$$

smoothly decreases at the high- q region without oscillation in momentum space. To see this, we examined typical cases for ^{12}C and ^{208}Pb nuclei. We assumed the charge distribution for ^{12}C as

$$\rho(r) = \frac{2Ze}{\pi^{3/2}a^3(2+3b)} \left[1 + b \left(\frac{r}{a}\right)^2 \right] \exp\left[-\left(\frac{r}{a}\right)^2\right], \quad (9)$$

then the Coulomb potential is given by

$$V(r) = \frac{8Ze^2}{\sqrt{\pi}a^3(2+3b)} \left\{ -\frac{ba^2}{4} \exp\left[-\left(\frac{r}{a}\right)^2\right] + \frac{\sqrt{\pi}a^3}{4} \left(1 + \frac{3b}{2} \right) \frac{\text{erf}(r/a)}{r} \right\}, \quad (10)$$

with $a = 1.66$ fm and $b = 1.33$ fm. For the case of ^{208}Pb , we assumed the charge distribution

$$\rho(r) = \rho_0 \left/ \left\{ 1 + \exp\left[\frac{r-c}{t}\right] \right\} \right. \quad (11)$$

We used the parameters $c = 6.46$ fm and $t = 0.542$ fm. These Coulomb potentials are expanded as in Eq. (7) in terms of the Gaussian functions. We used the radius parameter $R = 7$ fm for ^{12}C and $R = 13$ fm for ^{208}Pb , respectively. The optimal parameters c_i and λ_i were searched, and the expansions with $N = 5$ and $N = 7$ terms were found to be sufficient for ^{12}C and ^{208}Pb , respectively. In Fig. 1, we show the Coulomb potential and the regularized one $\bar{V}(r)$ represented by the superposition of the Gaussian functions as in Eq. (8). As seen, the Coulomb potential at the region $r \leq R$ is well described as the superposition of the Gaussian functions, providing us with a smooth-cutoff Coulomb potential. The difference between $V(r)$ and $\bar{V}(r)$ at $r \leq R$ are, at most, 0.27% for ^{12}C and 0.12% for ^{208}Pb , respectively. These are accu-

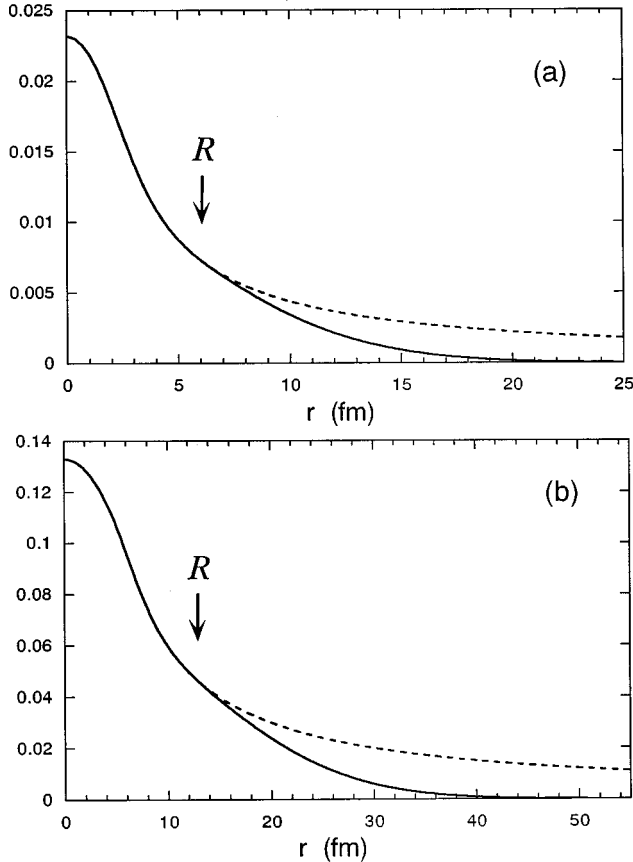


FIG. 1. The dashed lines represent the Coulomb potential for (a) proton- ^{12}C and (b) proton- ^{208}Pb , respectively. The solid lines are the regularized Coulomb potential $\bar{V}(r)$ described in the text.

rate enough for our present purpose. If more accuracy were needed, the number of Gaussian terms could be increased. To demonstrate the behavior in momentum space, we show the Fourier transform of the Coulomb potential for ^{12}C in Fig. 2. The Fourier transform of the regularized Coulomb potential corresponds to the solid line, decreasing rapidly without oscillation. For comparison, we show the sharp-cutoff Coulomb potential by VP procedure as well as the shielded potential used by Ottenstein *et al.* [11,12] with parameters $R_{\text{sh}}=14$ fm and $a_{\text{sh}}=2$ fm. As previously indicated, the sharp-cutoff Coulomb potential oscillates rapidly and decreases slowly as $1/q^2$, giving large high- q components. On the other hand, the shielded Coulomb potential by Ottenstein *et al.* [11,12] decreases rapidly due to the exponential factors in Eq. (6) and is similar to the Fourier transform of our potential $\bar{V}(r)$. In the shielded potential by Ottenstein *et al.* [11,12], however, there are small but non-negligible oscillating components coming from the second term in Eq. (6) and, for this reason, the partial-wave decomposition has to be done carefully to avoid the cancellation of the integrand. In Ref. [12], this decomposition was carried out by numerical integration of 192 Gaussian points.

It should be stressed that there are no oscillatory components in our regularized Coulomb potential. Moreover, the partial-wave decomposition can be done analytically as

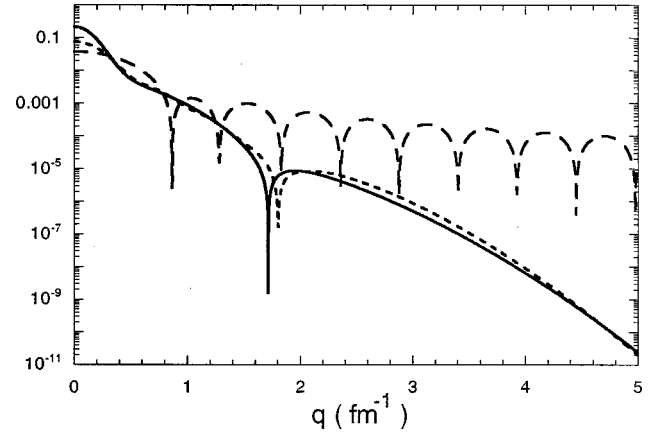


FIG. 2. The Fourier transform of the Coulomb potential for ^{12}C . The long-dashed curve corresponds to the sharp-cutoff Coulomb potential which is used by Vincent and Phatak [1]. The short-dashed curve is the shielded Coulomb potential (6) which was used by Ottenstein *et al.* [11,12] with the parameters $R_{\text{sh}}=14$ fm and $a_{\text{sh}}=2$ fm. The solid line is the regularized Coulomb potential expanded as the superposition of the Gaussian functions used in the present work.

$$\bar{V}_L(k, k') = \frac{1}{2\sqrt{\pi}} \sum_{i=1}^N c_i / \lambda_i^{3/2} \exp\left[-\frac{k^2 + k'^2}{4\lambda_i}\right] i_L\left(\frac{kk'}{2\lambda_i}\right), \quad (12)$$

where $i_L(x)$ is the modified spherical Bessel function. To test our algorithm, we used the simplified proton-nucleus optical potential of the following form:

$$U(r) = V_0 \left[1 + c_s \left(\frac{r}{d_s} \right)^2 \right] \exp\left[-\left(\frac{r}{d_s} \right)^2 \right], \quad (13)$$

with the parameters $c_s=1.33$ and $d_s=1.57$ fm for ^{12}C and $c_s=1.98$ and $d_s=3.94$ fm for ^{208}Pb . We adopt the potential depths $V_0 = -50, -15,$ and -5 MeV for incident energies $T_p = 50, 150,$ and 250 MeV, respectively. These are close to the values of the global nucleon-nucleus optical potential [17–19]. The imaginary parts are neglected. Even though these parameters do not describe the realistic proton-nucleus elastic scattering precisely, their major purpose is to examine the validity of the numerical algorithm, and we thus chose to use these parameters throughout. The Lippmann-Schwinger integral equation in each partial wave

$$(k_0^2 - k^2) \psi_L(k) = 2M \int_0^\infty [U_L(k, k') + \bar{V}_L(k, k')] \psi_L(k') k'^2 dk', \quad (14)$$

can be solved by discretizing the integral equation and using the matrix inversion method [20]. In the above equation, $\bar{V}(r)$ is the partial-wave component of the regularized Coulomb potential in Eq. (12). In order to calculate the phase shifts from Eq. (14), we used two algorithms:

TABLE I. The phase shifts δ_L for proton- ^{12}C elastic scattering at incident energy T_p . The results calculated in coordinate space (r space) and momentum space (k space) are compared. For the momentum-space calculation, two methods (I) and (II) are used which are described in the text.

T_p	L	$\delta_L(\text{degree})$			$\delta_L(\text{degree})$			
		r space	k space (I)	k space (II)	L	r space	k space (I)	k space (II)
50.0 MeV	0	-78.614	-78.609	-78.609	4	14.896	14.904	14.904
	1	88.760	88.763	88.763	5	3.861	3.877	3.877
	2	73.806	73.814	73.814	6	0.902	0.901	0.901
	3	44.442	44.433	44.434	7	0.190	0.190	0.191
150.0 MeV	0	26.545	26.546	26.546	5	8.060	8.061	8.061
	1	21.843	21.847	21.847	6	4.913	4.910	4.911
	2	18.740	18.742	18.742	7	2.682	2.684	2.684
	3	15.478	15.483	15.483	8	1.325	1.332	1.332
	4	11.785	11.784	11.784	9	0.598	0.603	0.603
250.0 MeV	0	12.367	12.369	12.369	6	2.788	2.787	2.787
	1	8.929	8.930	8.930	7	1.966	1.966	1.966
	2	7.162	7.165	7.165	8	1.304	1.302	1.303
	3	5.877	5.878	5.879	9	0.813	0.814	0.815
	4	4.765	4.767	4.767	10	0.476	0.479	0.479
	5	3.734	3.734	3.734	11	0.263	0.266	0.266

(I) The radius parameter R_m is denoted such that $\bar{V}(r) \sim 0$ for $r \geq R_m$. First, we calculate the phase shifts $\delta_L^{(0)}$ from Eq. (14). Starting from the coordinate-space wave function at $r \geq R_m$,

$$F_L(k_0 r, \eta=0) + \tan \delta_L^{(0)} G_L(k_0 r, \eta=0), \quad (15)$$

the coordinate space wave equation with the potential $\bar{V}(r)$ is solved inward to R . Subsequently, the logarithmic derivative at $r=R$ is matched with

$$F_L(k_0 r, \eta) + \tan \delta_L G_L(k_0 r, \eta), \quad (16)$$

and the correct phase shifts δ_L are obtained. Here, F_L and G_L are the regular and irregular Coulomb wave functions [21]. This procedure is similar to that used by Ottenstein *et al.* [11,12].

(II) From Eq. (14), we obtain momentum-space wave function $\psi_L(k)$, from which the coordinate-space wave function is calculated by the Fourier transform. Then the logarithmic derivative at $r=R$ is directly matched to the Coulomb wave function (16) to reproduce the correct phase shifts δ_L .

To carry out the practical calculation, the momentum-space grid points and weights have to be selected adequately to discretize the integral in Eq. (14). Since our regularized Coulomb interaction $\bar{V}(r)$ has a long tail, as shown in Fig. 1, its Fourier transform exhibits a narrow peak around k_0 in momentum space, especially for the case of ^{208}Pb . Considering the behavior of the potential matrix elements, we divide the whole integral interval $0 < k < \infty$ into four parts and adopt the following mappings with Gaussian points $-1 < x_i < 1$ and weights w_i :

$$(a) 0 \leq k \leq (1 - \varepsilon)k_0,$$

$$k_i = \frac{1 - \varepsilon}{2} k_0 (1 + x_i), \quad (17)$$

$$z_i = \frac{1 - \varepsilon}{2} k_0 w_i.$$

$$(b) (1 - \varepsilon)k_0 \leq k \leq (1 + \varepsilon)k_0,$$

$$k_i = (1 + \varepsilon x_i) k_0, \quad (18)$$

$$z_i = \varepsilon k_0 w_i.$$

$$(c) (1 + \varepsilon)k_0 \leq k \leq 2k_0,$$

$$k_i = \frac{1 - \varepsilon}{2} k_0 x_i + \frac{3 + \varepsilon}{2} k_0, \quad (19)$$

$$z_i = \frac{1 - \varepsilon}{2} k_0 w_i.$$

$$(d) 2k_0 \leq k \leq \infty,$$

$$k_i = \frac{2(3 + x_i)}{1 - x_i} k_0, \quad (20)$$

$$z_i = \frac{8k_0}{(1 - k_i)^2} w_i.$$

Interval (b) corresponds to the large Fourier component coming from the long-range regularized Coulomb potential. We adjust the parameter ε ($0 < \varepsilon < 1$) to accommodate the Fourier component around the on-shell value k_0 . For the case of

TABLE II. The same as those in Table I but for ^{208}Pb .

T_p	L	r space	δ_L (degree)		L	r space	δ_L (degree)	
			k space (I)	k space (II)			k space (I)	k space (II)
50.0 MeV	0	-75.811	-75.816	-75.814	10	47.301	47.255	47.256
	1	42.979	42.975	42.977	11	22.204	22.238	22.240
	2	-0.256	-0.268	-0.267	12	10.647	10.671	10.673
	3	-34.770	-34.761	-34.759	13	5.142	5.134	5.136
	4	-66.028	-66.028	-66.026	14	2.443	2.426	2.428
	5	82.541	82.555	82.557	15	1.113	1.102	1.103
	6	48.770	48.760	48.761	16	0.474	0.470	0.472
	7	10.700	10.662	10.663	17	0.186	0.185	0.187
	8	-32.811	-32.786	-32.785	18	0.066	0.065	0.067
9	-85.089	-85.074	-85.073	19	0.021	0.020	0.022	
150.0 MeV	0	25.908	25.905	25.909	10	46.795	46.773	46.780
	1	-20.416	-20.427	-20.419	11	40.051	40.042	40.046
	2	-47.758	-47.765	-47.761	12	33.738	33.742	33.749
	3	-66.521	-66.532	-66.525	13	27.945	27.957	27.964
	4	-80.681	-80.684	-80.679	14	22.752	22.768	22.773
	5	87.876	87.875	87.882	15	18.208	18.204	18.213
	6	78.120	78.123	78.128	16	14.327	14.309	14.314
	7	69.431	69.430	69.436	17	11.083	11.058	11.063
	8	61.435	61.423	61.429	18	8.426	8.394	8.403
9	53.922	53.907	53.912	19	6.298	6.275	6.282	
250.0 MeV	0	-31.835	-31.841	-31.835	10	25.915	25.905	25.913
	1	-71.039	-71.048	-71.041	11	22.492	22.480	22.486
	2	86.953	86.944	86.950	12	19.445	19.430	19.437
	3	72.077	72.066	72.074	13	16.728	16.711	16.718
	4	61.013	61.004	61.010	14	14.308	14.298	14.303
	5	52.311	52.305	52.312	15	12.158	12.152	12.159
	6	45.211	45.207	45.214	16	10.263	10.266	10.272
	7	39.266	39.267	39.273	17	8.605	8.615	8.621
	8	34.187	34.184	34.192	18	7.170	7.176	7.184
9	29.782	29.780	29.786	19	5.938	5.944	5.949	

^{12}C , the results of the momentum-space calculation are rather insensitive to the choice of the parameter ε . On the other hand, the results are fairly dependent on the choice of ε for ^{208}Pb . This is because the regularized Coulomb potential for ^{208}Pb has a long tail reaching to about 40 fm, which brings a narrow peak structure to the momentum-space Coulomb matrix element. We use the parameter $\varepsilon = 0.2$ throughout the present work for both ^{12}C and ^{208}Pb .

The results of the calculation for the phase shifts are shown as k space in Tables I and II for the cases of ^{12}C and ^{208}Pb , together with the results of the coordinate-space calculation denoted as r space. We have adopted the grid points 40,30,30,40 for the interval (a)-(d), respectively. The coordinate-space calculation has been carried out with the Bulirsh-Stoer method [22], which is known to be quite accurate for solving ordinary differential equations. In the momentum-space calculation, we adopt the two algorithms described above. As shown in these tables, the momentum-space calculations (I) and (II) yield almost the same results. For both of the momentum-space methods (I) and (II), the

above-mentioned grid points are enough to obtain accurate results. For the momentum-space method (I), a smaller number of grid points are sufficient to obtain accurate results. This is because the method (II) is directly related to the coordinate-space wave function, while only its asymptotic behavior (i.e., $\tan \delta_L^{(0)}$) is relevant to method (I). This indicates that, if accurate wave functions are necessary to calculate some nuclear matrix elements, enough grid points also need to be taken in momentum-space calculation. For the case of ^{12}C , the difference between coordinate-space and momentum-space calculations is less than 0.01 degree. The average differences are about 0.005 degree at $T_p = 50$ MeV and 0.002 degree at $T_p = 250$ MeV. For ^{208}Pb , the average difference of the phase shifts between r -space and k -space calculations is about 0.01 degree at $T_p = 50$ MeV and 0.008 degree at $T_p = 250$ MeV. With the method of Ottenstein *et al.*, the phase shifts calculated in r space and k space typically agree better than 0.5 degree [12]. The present method is quite accurate without tedious numerical calculation. At higher energies, we have also calculated the phase shifts at

incident energy $T_p = 500$ MeV and have checked that we can obtain similar accuracy.

As mentioned above, there is no subtle numerical integration in our method for the partial-wave decomposition of the regularized Coulomb potential. It is very easy to obtain accurate Coulomb matrix elements even for large k or k' , where partial-wave projection has been difficult with the methods used so far. In the practical calculation, the exponential dependence of the modified spherical Bessel function is extracted as

$$\begin{aligned} \bar{V}_L(k, k') = & \frac{1}{2\sqrt{\pi}} \sum_{i=1}^N c_i / \lambda_i^{3/2} \exp\left[-\frac{(k-k')^2}{4\lambda_i}\right] \\ & \times \left[\exp\left(-\frac{kk'}{2\lambda_i}\right) i_L\left(\frac{kk'}{2\lambda_i}\right) \right], \end{aligned} \quad (21)$$

then, for large $x = kk'/2\lambda_i$, the function $[\exp(-x)i_L(x)]$ slowly decreases and can be easily calculated by the series expansion with respect to $1/x$. Thus, the numerical difficulties inherent in the original VP procedure are overcome, and accurate numerical results could be obtained.

III. CONCLUSIONS

We have developed an improved algorithm to treat the Coulomb interaction in momentum space for the scattering problem. In the original VP procedure, the sharp-cutoff Coulomb potential is used. It brings an oscillatory high- q component to the Coulomb potential which decreases slowly in momentum space. We propose to regularize the Coulomb potential by using the superposition of the Gaussian functions. This method has two advantages, namely that the momentum-space Coulomb potential rapidly decreases with-

out oscillation, and that the partial-wave decomposition of the Coulomb potential can be done analytically. We examined our algorithm for the typical cases of proton- ^{12}C and proton- ^{208}Pb elastic scatterings for $T_p = 50\text{--}250$ MeV. In the momentum-space calculation, we examined two methods:

(I) First, the phase shifts $\delta_L^{(0)}$ is calculated with the regularized Coulomb potential at R . Then, the asymptotic wave function is obtained in coordinate space at large r , where the cutoff Coulomb interaction almost vanishes $\bar{V}(r) \sim 0$. Starting from this, the coordinate-space wave equation is solved with the potential $\bar{V}(r)$ inward to R . Then, the logarithmic derivative at $r=R$ is matched to the Coulomb wave function, and the correct phase shifts δ_L can be reproduced.

(II) From the momentum-space wave equation with the potential $U_L(k, k') + \bar{V}_L(k, k')$, the wave function $\psi_L(k)$ is obtained, from which the coordinate-space wave function is calculated by the Fourier transform. Then the logarithmic derivative at $r=R$ is directly matched to the Coulomb wave function to reproduce the correct phase shifts δ_L .

As a numerical test for our algorithm, we have calculated the phase shifts for the proton-nucleus elastic scattering with the optical potential plus Coulomb potential for ^{12}C and ^{208}Pb . We have shown that we can obtain accurate results for both cases over a wide energy region. The numerical difficulties inherent in the original VP procedure having been thus overcome, and we could easily treat the long-range Coulomb force in momentum space.

ACKNOWLEDGMENTS

We would like to thank Professor H. Horiuchi for stimulating discussions. This work was supported by Grant-in-Aid for Scientific Research (No. 08640376) from Japan Ministry of Education, Science, and Culture.

-
- [1] C.M. Vincent and S.C. Phatak, Phys. Rev. C **10**, 391 (1974), and references therein.
- [2] R.A. Eisenstein and F. Tabakin, Comput. Phys. Commun. **12**, 237 (1976).
- [3] R.A. Eramzhyan, M. Gmitro, and S.S. Kamalov, Phys. Rev. C **41**, 2865 (1990).
- [4] A. Cieply, M. Gmitro, R. Mach, and S.S. Kamalov, Phys. Rev. C **44**, 713 (1991).
- [5] R. Crespo and J.A. Tostevin, Phys. Rev. C **41**, 2615 (1990).
- [6] A. Picklesimer, P.C. Tandy, R.M. Thaler, and D.H. Wolfe, Phys. Rev. C **30**, 1861 (1984).
- [7] H.F. Arellano, F.A. Brieva, and W.G. Love, Phys. Rev. C **41**, 2188 (1990).
- [8] R.A. Eisenstein and F. Tabakin, Phys. Rev. C **26**, 1 (1982).
- [9] C.R. Chinn, Ch. Elster, and R.M. Thaler, Phys. Rev. C **44**, 1569 (1991).
- [10] D.H. Lu, T. Mefford, R.H. Landau, and G. Song, Phys. Rev. C **50**, 3037 (1994).
- [11] N. Ottenstein, E.E. van Faassen, J.A. Tjon, and S.J. Wallace, Phys. Rev. C **42**, R1825 (1990).
- [12] N. Ottenstein, E.E. van Faassen, J.A. Tjon, and S.J. Wallace, Phys. Rev. C **43**, 2393 (1991).
- [13] K. Dreissigacker, H. Pöpping, P.U. Sauer, and H. Walliser, J. Phys. G **5**, 1199 (1979).
- [14] Ch. Elster, L.C. Liu, and R.M. Thaler, J. Phys. G **19**, 2123 (1993).
- [15] E.O. Alt and W. Sandhas, Phys. Rev. C **21**, 1733 (1980).
- [16] E.O. Alt, W. Sandhas, and H. Ziegelmann, Nucl. Phys. **A445**, 429 (1985).
- [17] R.L. Varner, W.J. Thompson, T.L. McAbee, E.J. Ludwing, and T.B. Clegg, Phys. Rep. **201**, 57 (1991).
- [18] A. Ingemarsson, O. Jonsson, and A. Hallgren, Nucl. Phys. **A319**, 377 (1979).
- [19] K.W. Jones *et al.*, Phys. Rev. C **50**, 1982 (1994).
- [20] R.A. Eisenstein and F. Tabakin, Comput. Phys. Commun. **12**, 237 (1976).
- [21] A.R. Barnett, D.H. Feng, J.W. Steed, and L.J.B. Goldfarb, Comput. Phys. Commun. **8**, 377 (1974).
- [22] W.H. Press, B.P. Flannery, S.A. Teukolsky, and W.T. Vetterling, *Numerical Recipes*, (Cambridge University Press, Cambridge, 1989), Chap. 15.4, p. 563.